J. Fluid Mech. (1978), *vol.* 89, *part* 1, *pp.* 147–171
Printed in Great Britain

The effect of a transverse magnetic field on shear turbulence

By CLAUDE B. REED† AND PAUL S. LYKOUDIS

School of Nuclear Engineering, Purdue University,
West Lafayette, Indiana 47907

(Received 30 May 1977 and in revised form 22 February 1978)

Turbulence measurements under the influence of a transverse magnetic field have been made at Purdue University's Magneto-Fluid-Mechanic Laboratory in a high aspect ratio channel. The Reynolds number range covered was $25000 \leqslant Re \leqslant 282000$; the geometry and experimental conditions were such that the experiment approximated turbulent Hartmann flow. The aspect ratio of the channel was 5·8 : 1, its walls were electrically insulated and the working fluid was mercury. Measurements in the presence of a magnetic field were made of the skin friction coefficient, the mean velocity profiles, the turbulence intensity profiles (both u' and v') and the Reynolds stress profiles.

A sudden change in the damping of the Reynolds stresses was manifested by a 'hump' in the curves of C_f versus M/Re taken with the Reynolds number held constant. This 'hump' occurs as a gentle rise and sudden drop to the Hartmann laminar line of the C_f data. Close examination of the $\overline{u'v'}$ data near the wall confirms this behaviour, indicating that the turbulent contribution to the shear stress is the controlling factor in this behaviour of C_f. The Reynolds stresses were completely suppressed to zero at high values of the magnetic field, though the turbulence intensities of u' and v' were not. The Reynolds stress data are fundamental in revealing the mechanisms which are at work during the suppression of turbulence by a magnetic field.

It was also found that at high magnetic fields, when most of the turbulence was damped, the skin friction coefficient fell below the values predicted by Hartmann's (1937) laminar solution for high values of M/Re. This result was linked to the presence of 'M-shaped' velocity profiles in the direction perpendicular to both the magnetic field and the mean velocity vector. The presence of 'M-shaped' profiles has not previously been linked to a reduction in C_f.

1. Introduction

There is considerable renewed interest in the area of liquid-metal Magneto-Fluid-Mechanic (MFM) flow in the area of MHD power generation and also in conceptual designs of proposed blankets of fusion reactors. As is the case in ordinary fluid mechanics (OFM), most MFM fluid flows of practical interest are turbulent. Hence we are faced with the problem of studying the effect of a magnetic field on turbulent flow.

This paper presents the results of the latest work in a series of experiments beginning with Brouillette (1966) and continuing with Hua (1968), Gardner (1969), Papailiou

† Present address: Argonne National Laboratory, Argonne, Illinois 60439.

& Lykoudis (1974), Patrick (1976) and Reed (1976). These experiments concerned themselves with measuring and understanding the behaviour of shear turbulence in the presence of magnetic fields.

2. The experiment

2.1. *The channel*

To approximate the flow between infinite parallel plates, a high aspect ratio channel (5·82 : 1) was used. The internal measurements of the channel were 8 inches ($= 2w$) in the wide direction (z), 1·375 inches ($= 2d$) in the y direction (B and Oy were vertical), and 10 feet in the axial direction (x). The y direction was the transverse direction. This configuration provided 30 hydraulic diameters of entrance length for the fluid prior to reaching the magnetic field. An abrupt transition from the circular cross-section of the loop piping to the rectangular cross-section of the channel was made of stainless steel and Plexiglas and was approximately 6 inches in length.

The channel was essentially a modification of the channel used by Hua (1968). The channel was constructed of two materials, aluminium and Plexiglas. The Plexiglas was used to line the channel to achieve the insulated wall boundary condition.

The latter 50 inches of the channel were situated between the pole faces of a d.c. electromagnet. This length gave approximately 21 hydraulic diameters under the influence of the magnetic field.

The channel was instrumented with 15 side wall static pressure taps. These were used to measure the axial pressure gradient from which the skin friction coefficient, C_f, was calculated.

2.2. *The MFM loop*

The channel was bolted into a stainless steel closed loop through which the mercury was circulated continuously by a Goulds centrifugal pump. The pump could be powered by either a 3 horsepower motor equipped with a continuously variable speed gear box, or a 30 horsepower motor. The coarse flow rate was regulated by choosing the appropriate motor and pulley arrangement and the fine flow control was provided by a hand operated globe valve. Other components in the loop included a disposable cartridge filter, a heat exchanger and a cooling water pressure regulator. A square-edged orifice was used as the standard from which the electromagnetic flowmeter was calibrated.

The electromagnetic flowmeter was positioned directly downstream of the orifice plate and after being calibrated using the orifice plate, it was used throughout the experiment to measure the Reynolds number.

There were two bubble chambers, one at the inlet and one at the exit of the channel, to facilitate purging air from the test section. The loop was filled by pressurizing the storage tank with nitrogen and thus forcing the mercury up into the system.

2.3. *Equipment and instrumentation*

General. The d.c. electromagnet used was manufactured by Pacific Electric Motor Company and was water cooled. It was capable of producing a uniform field of up to 1·4 tesla over the area of its pole faces, which was 12×50 square inches. The air gap for the experiment described here was 3 inches. The magnet consumed a maximum of 600 amperes at 300 volts. Its cooling water supply was the same as that of the heat

exchanger. The magnet was calibrated by measuring the field and the accompanying voltage drop across a shunt resistor in series with the magnet.

The a.c. power which serviced the electronic equipment in the MFM Laboratory was passed through a voltage regulator. Because of the precise nature of the measurements being made, and the difficulty encountered when taking a calibration curve for the hot-film anemometers, a voltage regulator was found to be necessary. A Vidar 520 Integrating Digital Voltmeter (IDVM) was the backbone of the data acquisition equipment.

It quickly became apparent during the use of the hot-film anemometers that their bridge voltage was a strong function of the ambient mercury temperature. In fact, it was necessary to place a thermocouple bead at the same cross-section as that containing the hot-film sensors and approximately one inch away in the z direction to obtain proper temperature compensation. Also, the reference junction for this thermocouple was moved very close to the bead to minimize the length of thermocouple wire over which temperature gradients could exist. The thermocouple voltages were measured with the Vidar IDVM.

2.4. *Skin friction measurements*

In order to make skin friction measurements, two differential pressure measuring instruments were used. The first was a Meriam micromanometer, mercury–water differential pressure manometer. It was possible to read the height of its mercury–water meniscus to $\pm$ 0·001 inch. It was used for all the skin friction measurements with the exception of those at $Re = 53000$ and $Re = 102000$, where the pressure differences were too small for this instrument. It was also used to measure the pressure drop across the square-edged orifice when calibrating the electromagnetic flowmeter.

For $Re = 53000$ and $Re = 102000$, the pressure differences were measured with a Pace electronic differential pressure transducer. Whereas the range of the Meriam micromanometer was 0 to 30 inches of mercury approximately, the Pace could measure up to 1 inch of water differential. It was calibrated using an inclined tube alcohol manometer.

2.5. *Mean velocity measurements*

The mean velocity of the mercury was measured with three instruments. A Pitot tube was used first and its function was basically to obtain the relationship between the centre-line velocity of the channel and the voltage from the flowmeter, or equivalently the Reynolds number. The results of Branover *et al.* (1966) show that Pitot tube measurements are not altered by the magnetic field strengths used in this experiment, for our Pitot tube orifice size. The flowmeter voltage was measured with the Vidar IDVM and the dynamic pressure of the Pitot tube was measured with the Meriam micromanometer. This relationship was required when hot-film anemometry was later used and had to be calibrated. The relationship between the channel centre-line velocity and the flowmeter voltage was linear within the accuracy of the measurements involved over the range investigated ($25000 < Re < 250000$).

When an X-probe was introduced into the experiment and it was attempted to measure profiles of the mean velocity and the fluctuating quantities, several difficulties were encountered. There were two reasons for these difficulties, departure from

'cosine cooling' and the use of a sensor at an angle with respect to the mean velocity which was different from the angle at which the sensor was calibrated. Briefly, departure from cosine cooling occurs when a cylindrical hot-film sensor, which is inclined with respect to the mean velocity vector, is cooled not only by the component of the velocity vector which is perpendicular to its axis, but also by the component which is parallel to its axis. The extent to which departure from cosine cooling affects the heat transfer from a hot-film sensor, and ultimately the measured bridge voltage, is represented by an empirical parameter k which is a function of the Péclet number, Pe. The parameter k increases with decreasing Péclet number and this makes it very important in the present investigation because of the very low Prandtl number of mercury. Both effects were sorted out and accounted for. This major problem encountered in the data reduction is fully discussed by Reed (1976). See also Reed & Lykoudis (1977) for a discussion of the mean and fluctuating velocity measuring techniques used here. A brief but pointed review of the state of the art of point velocity measurements in turbulent MFM mercury flow can be found in Hunt & Moreau (1976). Some of the problems associated with liquid-metal MHD hot-film anemometry are recited by Malcolm (1975).

A traversing mechanism located the probe, either a Pitot tube or a hot-film sensor, at almost any y or z location in the cross-section. The region very near the walls could not be accessed because of the size of the probe being used. The closest approach in the y direction was $y/d = 0{\cdot}054$ and in the z direction was $z/w = 0{\cdot}070$. The probe was moved in the z direction by withdrawing it from the side of the channel along its shaft. Both the Pitot tube and the hot-film anemometer probe shafts had right-angle bends in them so that when they were inserted through the wall of the channel, they faced upstream. The y direction was traversed by rotating the probe shaft. The probe could be positioned within $\pm 0{\cdot}002$ inch in both the y and the z direction. All mean velocity profiles reported were measured using an X-array hot-film probe. This type of probe was used so that mean velocities, axial turbulence intensities and transverse turbulence intensities could all be measured simultaneously.

In this experiment, 80% of the length of the flow which was under the influence of the uniform magnetic field was upstream of the probe and the remaining 20% was downstream. According to the qualitative work presented by Branover (1974), this location should be far enough away from both the inlet and exit region disturbances to approximate fully developed flow closely. The anemometry used was of the constant-temperature type manufactured by Thermo Systems Inc. (TSI).

2.6. *Measurement of the fluctuating quantities*

An integrating mean-square circuit was used to reduce the present fluctuating data and thus the true mean square was obtained for the entire record length available. The record length just mentioned refers to the records obtained when the fluctuating bridge voltages were recorded on a Honeywell-7600 FM tape recorder. The signals from both sensors were recorded simultaneously on two of the fourteen tracks on one inch FM tape. The two bridge voltages underwent considerable signal conditioning before they were recorded onto the tape. The raw bridge voltage signals were passed through a TSI model 1057 signal conditioner which performed two functions, low pass filtering (< 2 kHz) and 'zero suppression'. Zero suppression involved subtracting the d.c. voltage variably in increments of one volt. The signal was then passed through

a summing amplifier with unit gain. The summer was used to add a variable negative d.c. voltage to the signal such that the resultant signal had virtually no d.c. component. This signal was then passed through a Honeywell d.c. amplifier. The gain of this amplifier was fixed at the highest value which did not saturate the tape recorder. There were two reasons for this elaborate signal conditioning. The first was to record the signal as accurately as possible. The second was to record the signal on FM tape without affecting any of the low frequency content of the signal. Since the capability existed to measure the true mean square of the signals for any record length, and also since the energy content of the turbulence in mercury is in the low frequency range, it was felt that every effort should be made to preserve the frequency content of the signals. See Reed (1976) and Reed & Lykoudis (1977) for further details.

The root mean square of four quantities was measured in order to determine $\overline{(u'^2)}^{\frac{1}{2}}$, $\overline{(v'^2)}^{\frac{1}{2}}$ and $\overline{u'v'}$. If we designate by e_1 the fluctuation of bridge voltage 1 and by e_2 that of bridge 2, then the four quantities were $\overline{(e_1^2)}^{\frac{1}{2}}$, $\overline{(e_2^2)}^{\frac{1}{2}}$, $\overline{((e_1+e_2)^2)}^{\frac{1}{2}}$ and $\overline{((e_1-e_2)^2)}^{\frac{1}{2}}$. Of course only three of these are independent quantities, but the fourth was measured and compared with its value as calculated using the other three. This provided a check on the overall accuracy of the fluctuation measurements.

The four r.m.s.'s were measured in the following way. The recorded signals were played back through a TSI model 1015C correlator. The correlator was used as a summing or differencing network and gave as output e_1, e_2, e_1+e_2, or e_1-e_2. This signal was operated upon by a true mean-square circuit, the resultant voltage was read by the Vidar IDVM, divided by the time interval, and by a calibration constant. The square root of the result was the final operation.

2.7. *Experimental conditions*

All of the experiments were performed nominally at room temperature. Five Reynolds numbers were investigated: 25000; 53000; 102000; 197000; and 282000. The highest four were used for the measurements of C_f, the lowest three were used when measuring mean and fluctuating velocities. With the maximum magnetic field strength being 1·34 tesla, Hartmann numbers up to 2075 could be obtained. The ratio $(M/Re) \times 10^4$ reached maximum values in excess of 100 for the low Re and in the neighbourhood of 80 for the highest Re used here. The centre-line velocity for the experimental conditions covered here ranged from 0·17 ft/s to 1·9 ft/s.

3. Results and discussion

The OFM results for each quantity measured are presented first. It was felt that good agreement in the OFM case was essential to assure that reliable and accurate data were being taken. It was during the acquisition of the $\overline{u'v'}$ data that it became clear that a new method of data reduction was required if the sensor was to be calibrated at an angle with respect to the velocity vector which is different from the angle at which the measurements are made. The MFM results, where possible, are compared with the results of other similar measurements. There were some inconsistencies and they are discussed. More details can be found in Reed (1976) and Reed & Lykoudis (1977).

3.1. *Skin friction data*

OFM results. The C_f for the two highest Re were measured using the micromanometer and the results corresponded to Prandtl's skin friction relation (Schlichting 1960)

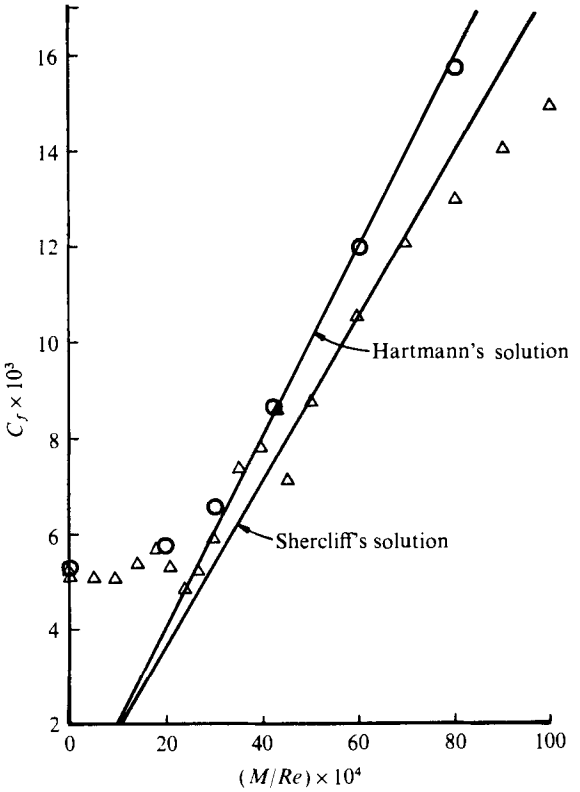

FIGURE 1. Skin friction data, $Re = 53000$. △, present data; ○, Bocheninski.

within approximately ± 2%. For one of four zero field measurements at $Re = 102000$, the C_f was 6·65% lower than Prandtl's relation. The C_f for $Re = 53000$ and 102000 were measured using a Pace differential pressure transducer. This good agreement supplied the confidence necessary to proceed with MFM measurements.

MFM results. The C_f results obtained are shown in figures 1 to 3. These results are very similar to the data presented by Hua (1968). See also Hua & Lykoudis (1975).

It can now be seen that the basic trends which appear in Hua's C_f data were reproduced. In addition to confirming these trends, the present work gives the explanation for this behaviour. This explanation can best proceed by considering the following two regions on the C_f graphs: $(M/Re) \times 10^4 \lesssim 30$ and $(M/Re) \times 10^4 \gtrsim 30$. The value of 30 was chosen as an approximate value which, for the Re involved in this experiment, seems to separate the behaviour of the skin friction coefficient into two regimes.

Figure 3 shows the C_f curve for $(M/Re) \times 10^4 \lesssim 30$ for $Re = 53000$. If we follow the data in the direction of increasing M/Re (increasing magnetic field), the data first dip slightly then rise to a local maximum in the neighbourhood of $(M/Re) \times 10^4 \simeq 18$–20. The minimum is the manifestation of the damping of the turbulence by the magnetic field. At Re lower than about 100000 to 180000, the minimum in the C_f curve is present because the Hartmann flattening effect cannot yet dominate the behaviour of the skin friction coefficient. The effect of the Hartmann flattening is to increase the shear stress at the wall and, therefore, the skin friction coefficient. The turbulence sup-

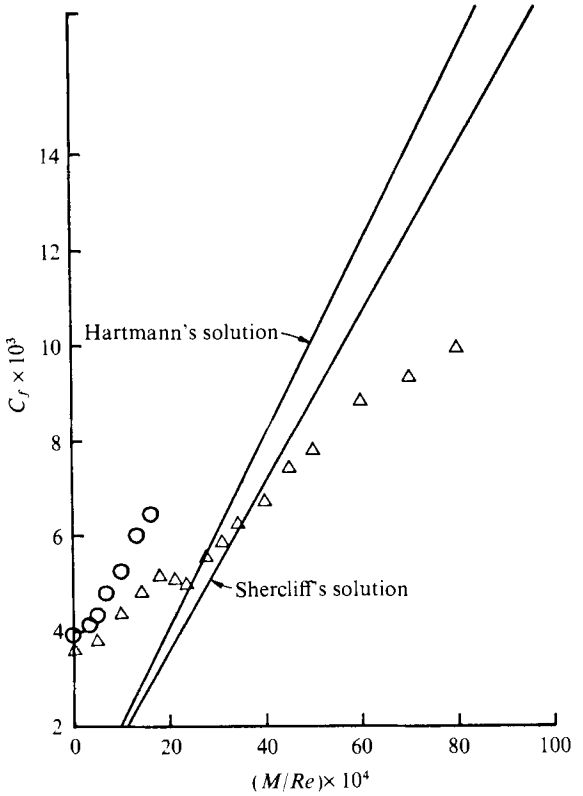

FIGURE 2. Skin friction data, $Re = 282000$. △, present data; ○, Bocheninski.

pression, on the other hand, tends to cut down the Reynolds stresses and therefore the wall stress, which decreases C_f. By looking at this portion of figures 1 to 3, one sees that the minimum vanishes as higher Re are reached. This minimum is well known and its disappearance with increasing Re was discovered by Brouillette & Lykoudis (1963). Hence, they found that eventually, at high enough Re, the Hartmann flattening effect always wins the battle against the turbulence suppression effect and C_f increases immediately upon application of the magnetic field.

Continuing to follow C_f in figure 3, we see a local maximum followed by a fairly sharp decrease in C_f. This local maximum, or 'hump', was also observed by Hua (1968) who stated that the same phenomenon could be found upon close examination in the work of both Murgatroyd (1953) and Brouillette & Lykoudis (1967). Considering the accuracy of skin friction data in general, one can only speculate as to the presence of a 'hump' in the data of Murgatroyd and Brouillette & Lykoudis. However, Gardner & Lykoudis (1971), who measured skin friction in a pipe, clearly found the 'hump' as did Maciulaitis & Loeffler (1964) also in a pipe. The latest C_f data available from the Soviet Union (Bocheninski *et al.* 1971) are also shown in figures 1 and 2. Their data were taken in channels of very high aspect ratio. Their data do not show the hump; in fact, they exhibit a trend of diverging above the 'Laminar Line'. The authors of that paper attribute this behaviour to an increase in the effective wall roughness in the presence of a magnetic field.

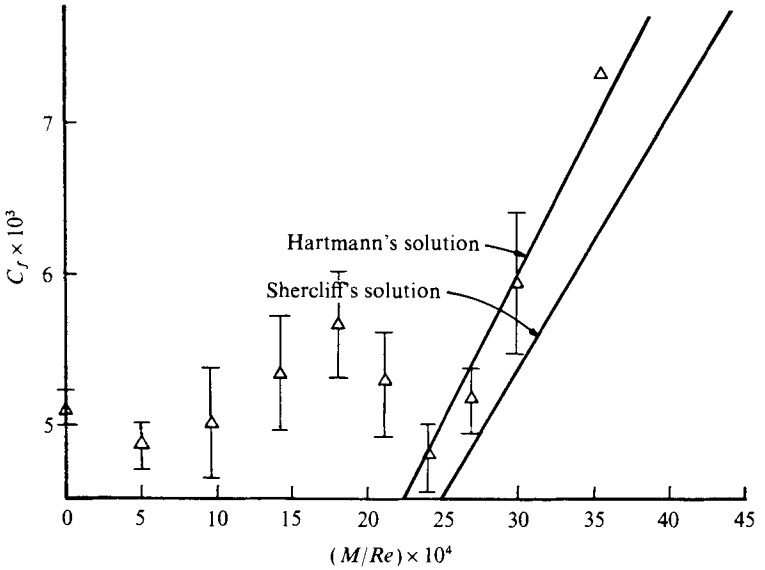

FIGURE 3. Low M/Re skin friction data, $Re = 53000$.

The argument put forth by Gardner & Lykoudis (1971) to explain the 'hump' in the C_f data links it to both the progressive suppression of the turbulence in the azimuthal direction and the transition from an essentially axisymmetric turbulent flow to a three-dimensional laminar flow.

The possibility of the presence of a substantial departure from two-dimensionality was investigated by measuring the mean velocity profiles in the transverse (z) direction. They are shown in figure 4 for $Re = 25000$, 53000 and 102000. One can see that for $(M/Re) \times 10^4 \lesssim 30$, the profiles in the transverse direction exhibit no unusual or unexpected behaviour. They are getting flatter owing to the Hartmann effect. There are a few points near the vertical side wall which have a slightly higher velocity than those at the centre-line. However, for the Re involved here and for $(M/Re) \times 10^4 \lesssim 30$ the transverse mean velocity profiles behave approximately as expected; they get flatter and flatter owing to the Hartmann effect.

Additional evidence that the flow has not become three-dimensional for

$$(M/Re) \times 10^4 \lesssim 30$$

and the Re under consideration here was found in the static pressure distribution measured across the width of the channel (figure 5). The distribution for

$$(M/Re) \times 10^4 = 29$$

and $Re = 282000$ was uniform across the width of the channel indicating that even at this high Re, the region below $(M/Re) \times 10^4 \simeq 30$ is free from three-dimensionality. It should be stated that the source of the 'hump' could not be experimental error as can be seen in figure 3 where the error bands resulting from a detailed error analysis are shown.

So far we have shown that the flow being dealt with does not suffer from three-dimensionality to the extent that could explain the 'hump'. We have also ascertained

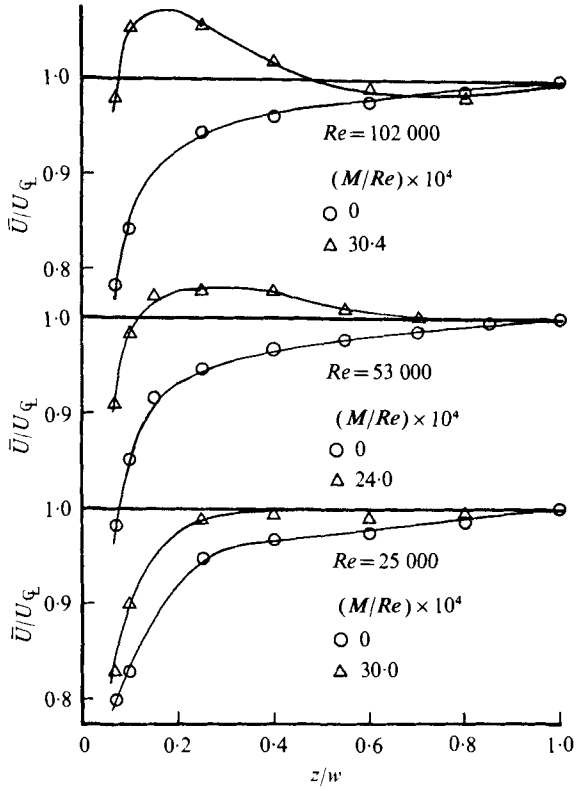

FIGURE 4. Transverse mean velocity profiles.

experimentally that the walls were electrically insulated. The explanation of the 'hump' can be found in the examination of the progress of the suppression of turbulence. If the shear stress at the wall decreases in the face of increased Hartmann flattening, the turbulent stress must be decreasing the wall stress faster than the Hartmann effect is increasing it. Figure 6 shows this description to be correct. Plotted in figure 6 is the turbulent stress $\rho\overline{u'v'}$ normalized by the wall stress u_τ^2 at measurement locations near the wall. The Re are 25000 and 53000. The abscissa is M/Re. It can be seen here that the damping of the turbulent stress becomes greatly accelerated beyond the value $(M/Re) \times 10^4 \approx 20$. This rapid change in damping rate causes the drop in C_f. Reynolds stress versus M/Re data exhibiting the same trend can also be found in the work of Patrick (1976) whose data were taken in a pipe.

Some parallels can also be drawn from the work of Papailiou & Lykoudis (1974). In that experiment, MFM temperature fluctuations were measured in the boundary layer of a heated vertical flat plate. Since the shear layer was much thicker there than in the present experiment, measurements could be made at smaller values of y^*. Papailiou's temperature fluctuation measurements near the edge of the laminar sublayer revealed an even more drastic suppression rate as transition to laminar flow was approached. This behaviour supports the assertion that near the wall, where the production of the turbulence is the greatest, the turbulence is only moderately suppressed by the magnetic field until the very final stages of transition where a very rapid rate of suppression is present.

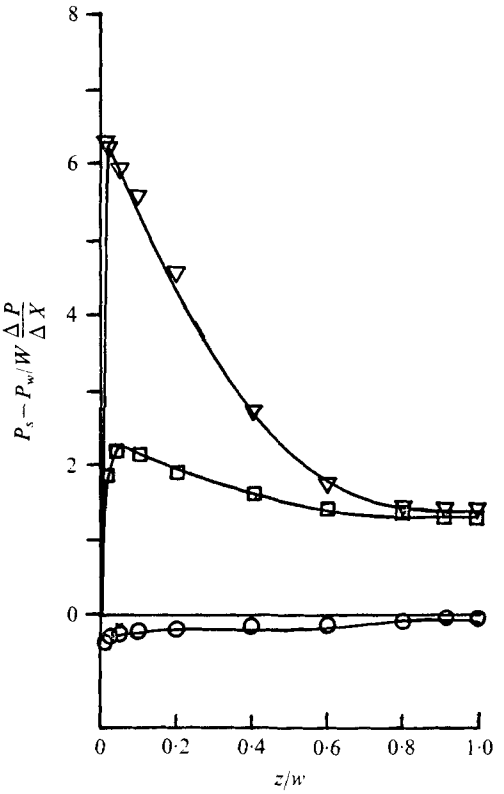

FIGURE 5. Static pressure distributions across width of channel showing 'M' shape, $Re = 282000$. $(M/Re) \times 10^4$: ▽, 100·0; □, 53·0; ○, 29·0.

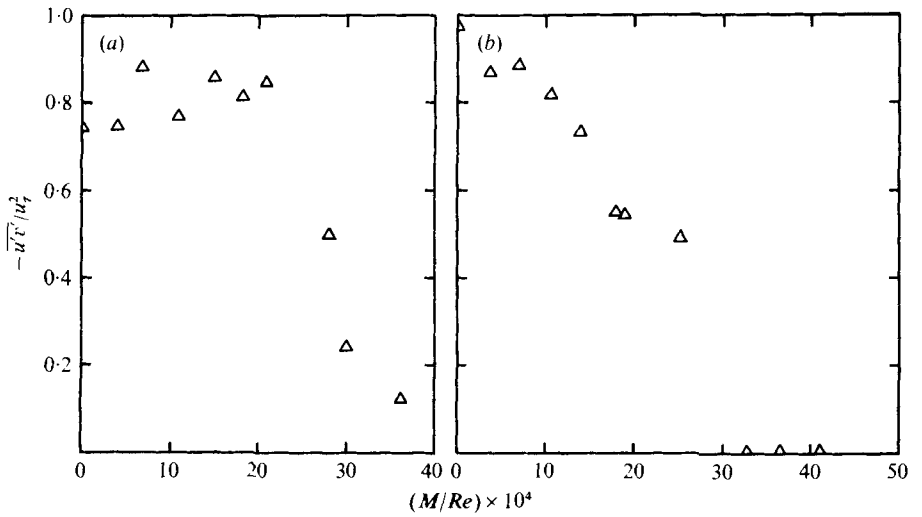

FIGURE 6. Experimental turbulent shear stress dependence on M/Re. (a) $Re = 25000$; $y^* = 40$; $y/d = 0{\cdot}1$. (b) $Re = 53000$; $y^* = 40$; $y/d = 0{\cdot}054$.

In summary, the following remarks can be made concerning C_f *vs.* M/Re for which $(M/Re) \times 10^4 \lesssim 30$. The present data exhibit a minimum in the C_f curve at low M/Re which vanishes for high Reynolds numbers. The present data also exhibit a 'hump' in the C_f data in the neighbourhood of $(M/Re) \times 10^4 \simeq 20$. The 'hump' is not a three-dimensional phenomenon because transverse velocity profiles indicate no unexpected three-dimensional behaviour in this range of M/Re; neither does it come from a violation of the electrically insulated wall boundary condition. The 'hump' is the result of the sudden, abrupt damping of the turbulent stress by the magnetic field in the neighbourhood of and beyond $(M/Re) \times 10^4 \approx 20$. Other data, namely the $\overline{u'v'}$ data, have been brought forth to explain the presence of the 'hump'. Data of other authors taken in both channels and pipes have been discussed which also display the same behaviour.

The discussion now turns to the region on the C_f *vs.* M/Re where $(M/Re) \times 10^4 \gtrsim 30$. Immediately it is seen that the data cross both laminar lines (figures 1 and 2) and fall below Shercliff's solution for the present aspect ratio. The explanation was first found when transverse (z direction) velocity profiles were measured with a Pitot tube and it was found that the velocity near the vertical side walls (parallel to B) was higher than the centre-line velocity when the magnetic field was sufficiently high. In fact, for one case measured here ($Re = 53000$; $(M/Re) \times 10^4 = 128$) the velocity near the wall was twice the centre-line value, figure 7. Examining this figure, it can be seen that the following is happening: as the magnetic field is increased to higher and higher values, the velocity near the vertical side walls (parallel to the field) increases to values higher and higher above the centre-line value. Because the flow rate was kept constant during these measurements, this velocity increase near the walls dictates a velocity decrease near the centre-line.

Figure 5 shows the static pressure distribution across the width of the channel at three values of M/Re for $Re = 282000$. The axial location of these profiles was the same as that of the velocity and turbulence intensity profiles. These static pressure profiles indicate that at high magnetic fields, there is quite a large pressure gradient in the z direction (here as large as 5 times the axial pressure gradient) which is attempting to force the fluid away from the walls parallel to the field, and toward the centre of the channel. This pressure distribution is trying to smooth out the M-shape of the velocity profiles.

This phenomenon is apparent in Lecocq (1964) though he did not mention it. It appeared but again went unmentioned in the data of Branover & Gel'fgat (1968). It was first mentioned by Branover, Gel'fgat & Tsinober (1966) in referring to Lecocq's (1964) work. Branover cited the work of Hunt (1965) which predicted bulges in the velocity profiles measured in the plane perpendicular to the field. However, Hunt's work predicted bulges only when the walls were electrical conductors, and in the data being referred to, as well as the remainder of the discussion on this subject, all of the walls are electrical insulators. Therefore, Hunt's solution will not do.

The first correct discussion of the phenomenon (bulges in the transverse velocity profiles) in the literature appeared in the work of Shercliff (1956). The author presented an approximate analysis which indicated that vorticity will be created at the inlet region of a magnetic field imposed on a channel of finite width.

Finally, in the work by Bocheninski *et al.* (1971), the M-shaped transverse velocity profiles were again measured and, in addition, detailed axial pressure distributions

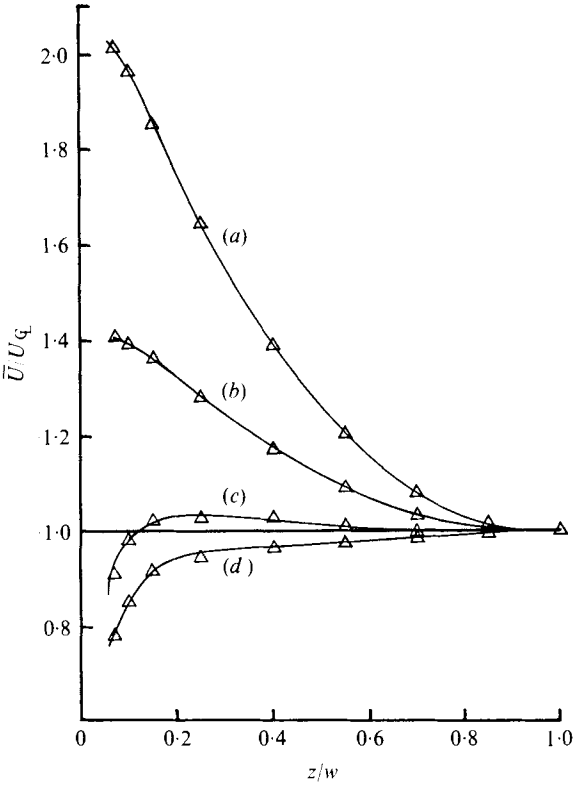

FIGURE 7. Transverse mean velocity profiles showing 'M-shaped' velocity distribution, Re = 53000. $(M/Re) \times 10^4$: (a) 127·0; (b) 69·0; (c) 24·0; (d) 0.

were presented. They were plagued with C_f data whose behaviour was opposite to that observed here. They found that their C_f data points fell *above* the laminar line, figures 3 to 6. They attributed this behaviour to an increase in the effective wall roughness resulting from the presence of the magnetic field, and rejected the hypothesis that the presence of M-shaped profiles affect C_f in any way. This assumption seems a bit more optimistic than the complexity of the problem warrants.

The explanation of the fact that the C_f data of Bocheninski *et al.* (1971) lie above the laminar line at high magnetic fields and the present C_f data lie below the laminar line is probably linked very intimately with the three-dimensionality of the flow.

It can be seen that the departure of the skin friction data from either Hartmann's solution or from Shercliff's solution will increase in an unpredictable way as, by increasing the magnetic field, the bulges become larger and larger. This unexpected three-dimensionality is clearly the explanation of the departure of the C_f data from their theoretically predicted asymptotic values.

3.2. *Mean velocity profiles*

OFM results. As mentioned earlier, the mean velocity measurements were obtained at the same time as the turbulence intensity fluctuations were being recorded on the tape recorder. All of the mean velocity measurements were obtained using the X-

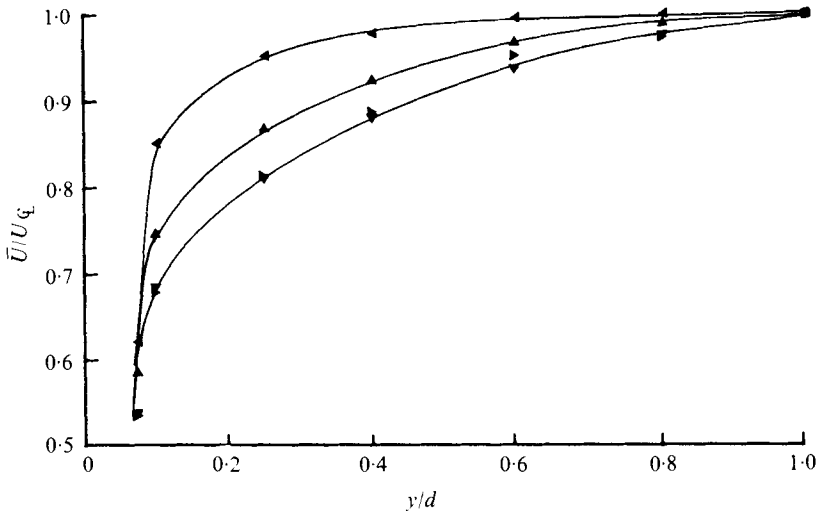

FIGURE 8. Mean velocity profile data in physical co-ordinates, $Re = 25000$. $(M/Re) \times 10^4$: ◀, 36·3; ▲, 20·7; ▶, 10·8, ▼, 0.

array hot-film sensors. The data were taken at three Reynolds numbers (Re = 25000, 53000, 102000) and at least nine non-zero magnetic field strengths.

The data were plotted in u^*, y^* co-ordinates and the least-squares method yielded the following relationship between u^* and y:

$$u^* = 6{\cdot}38 \log_{10} y^* + 3{\cdot}84.$$

Laufer (1950) found 6·9 for the slope and 5·5 for the intercept while Nickuradse (1929) found 5·75 and 5·5 respectively. Comte-Bellot (1965) commented that one can indeed find a wide variety of values for these two numbers in the literature.

The data follow the semi-logarithmic law very well, see Reed (1976). This good agreement with well known OFM results gave the authors confidence to go on to measure the mean and fluctuating velocities in the presence of a magnetic field.

MFM results. The velocity profiles under the influence of a magnetic field are shown in physical co-ordinates ($U/U_{\mathfrak{C}}$, y/d) in figures 8 and 9. The Hartmann flattening effect is very clear. The velocity profiles, unlike the skin friction data just presented, do not exhibit any unexpected or anomalous features. The velocity profiles are also cast in the u^*, y^* plane in figures 10 and 11.

A word is perhaps in order concerning the accuracy of the present data. Since the X-array hot-film probes used gave, in addition to the axial component of the velocity, the v component of the velocity, there was a built-in check on the accuracy of the measurements. Any non-zero value for the v component of the mean velocity was an indication that an error had crept into the measurements. The great majority of the velocity measurements taken indicated a v component smaller than $\pm 2\%$ of the axial centre-line velocity. For the data of Re = 25000 there were slightly higher errors but the majority of them were smaller than $\pm 3\%$ of the axial centre-line velocity.

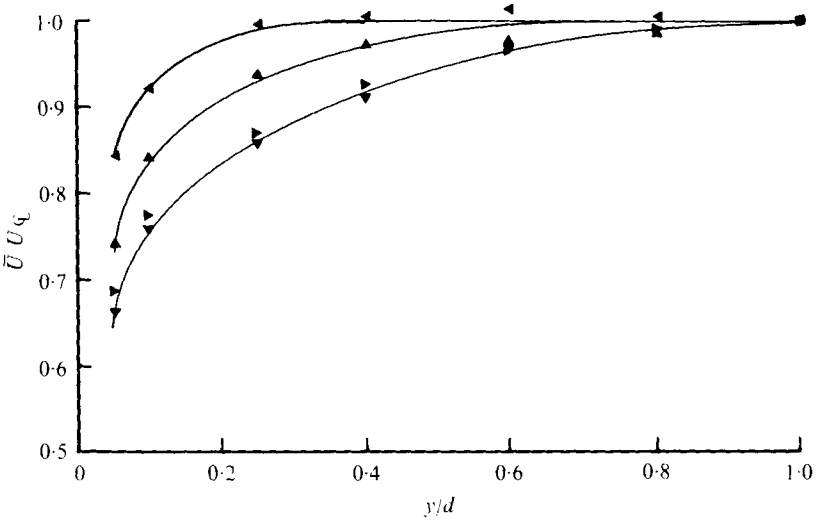

FIGUBE 9. Mean velocity profile data in physical co-ordinates, $Re = 102000$. $(M/Re) \times 10^4$: ◀, 17·1; ▲, 10·6; ▶, 7·1; ▼, 0.

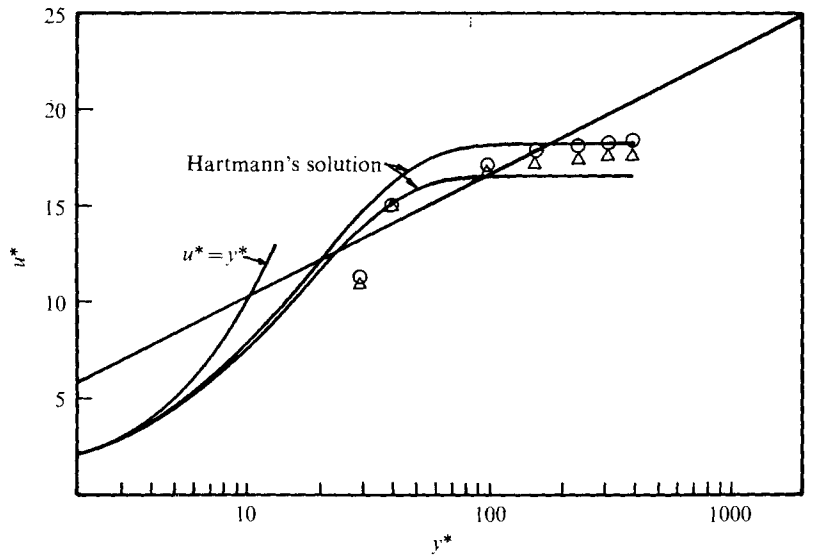

FIGURE 10. Mean velocity profile data in semi-logarithmic co-ordinates, $Re = 25000$. $(M/Re) \times 10^4$: △, 36·3; ○, 30·0.

3.3. *Turbulence intensity profiles*

OFM results. There are no theoretical or even semi-empirical predictions, of any merit, for the profiles of the intensity of u' or v' in the OFM case. This fact makes it very difficult to judge the quality or accuracy of turbulence intensity data. Laufer (1950), however, seems to have found that u' and v' data can be universalized, at least near the centre of a pipe or channel, if they are normalized by the friction velocity u_τ. For that reason, the present data are given in $(\overline{u'^2}/u_\tau)^{\frac{1}{2}}$ *vs.* y/d co-ordinates. Figure 12

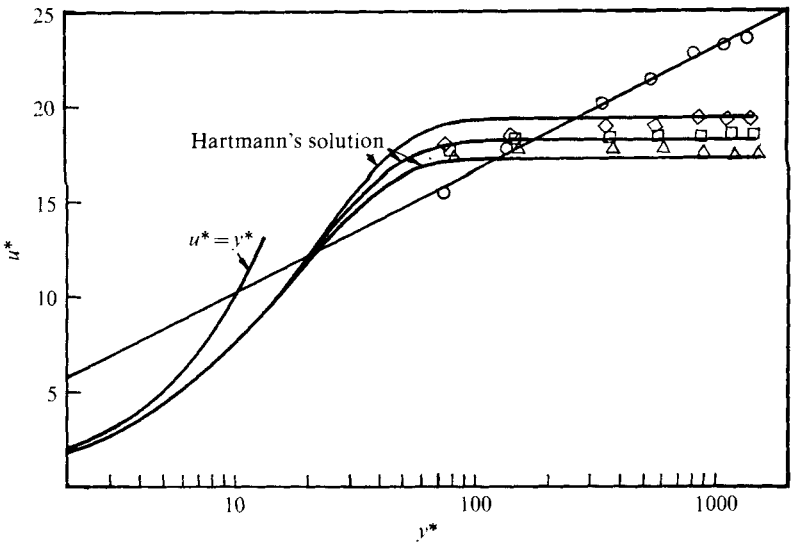

FIGURE 11. Mean velocity profile data in semi-logarithmic co-ordinates, $Re = 102000$. $(M/Re) \times 10^4$: ○, 0; ◇, 26·6; □, 30·2; △, 33·6.

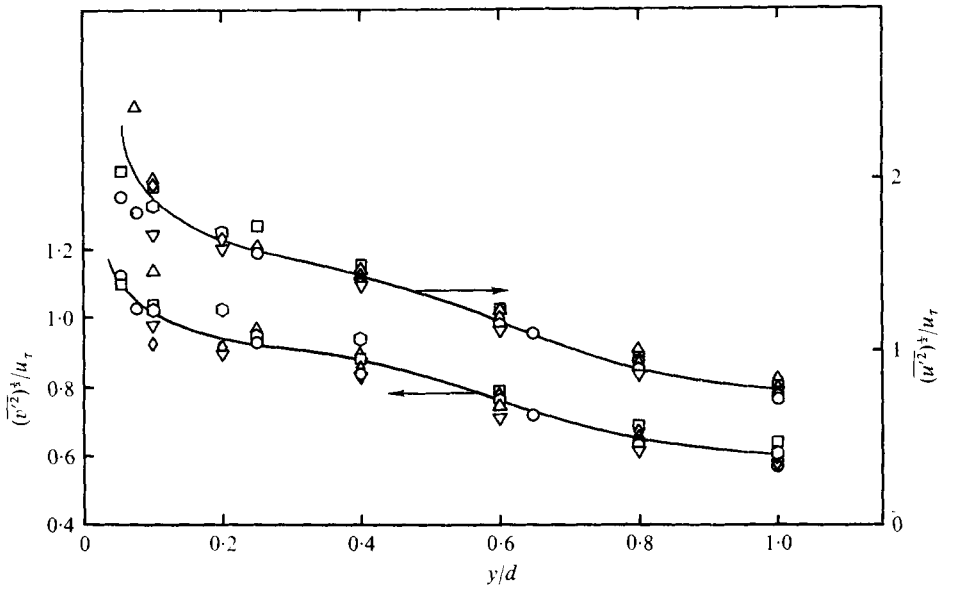

FIGURE 12. Comparison of present axial and transverse turbulence intensity profiles with those of Laufer. Reed Re: △, 25000; ○, 53000; □, 102000. Laufer Re: ◇, 12300; ⬡, 30800; ▽, 61600.

displays the present data at zero field along with Laufer's (1950) data. There is good agreement among all the data on the figure. The divergence of the points near the wall can be explained by considering the size of the probes used in the present experiment compared with the very small probes used by Laufer. Laufer was able to take data at points well into the laminar sublayer. This was not possible in the present work and some influence from the probe being near the wall was observed. The extent to which

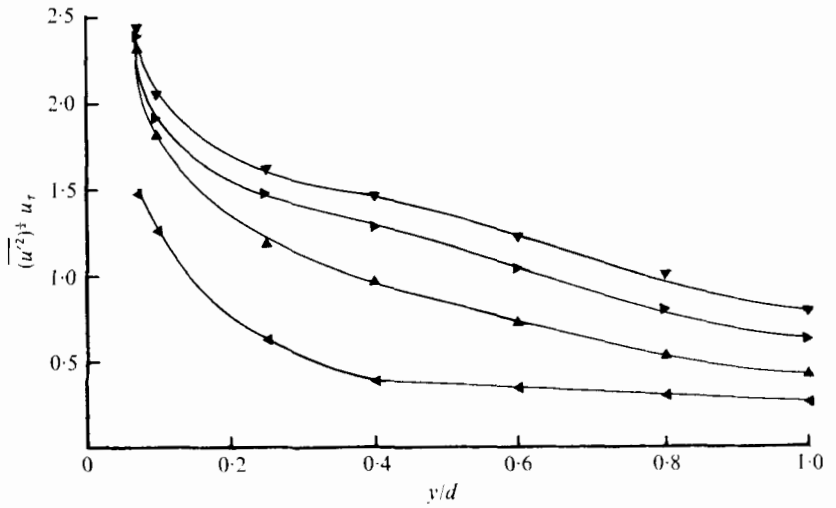

FIGURE 13. Present axial MFM turbulence intensity profiles, $Re = 25000$. $(M/Re) \times 10^4$: ◀, 36·3; ▲, 20·7; ▶, 10·8; ▼, 0.

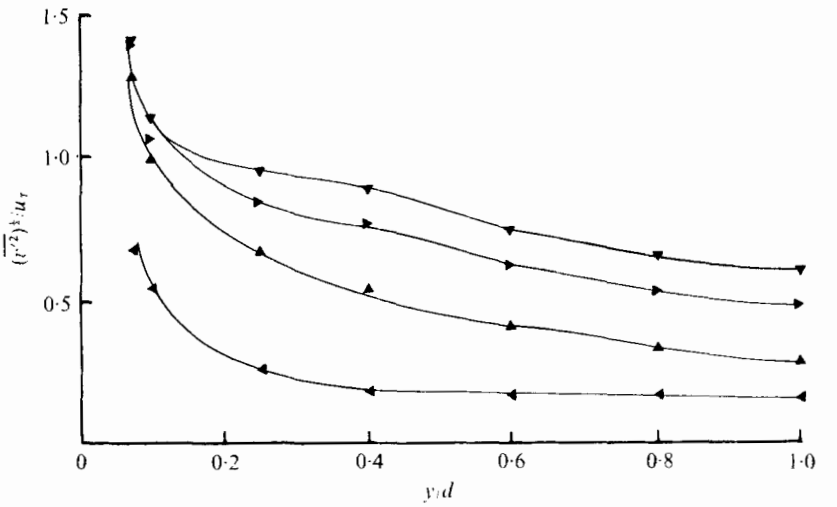

FIGURE 14. Present transverse MFM turbulence intensity profiles, $Re = 25000$. $(M/Re) \times 10^4$: ◀, 36·3; ▲, 20·7; ▶, 10·8; ▼, 0.

the present results were affected by the amplitude attenuation and phase lag associated with hot-film sensors in liquid-metals, as discussed in the works of Malcolm & Verma (1973) and Sleicher & Lim (1973), was estimated as follows. The criteria developed by Malcolm & Verma (1973) and Sleicher & Lim (1973) were evaluated and compared with Gardner & Lykoudis' (1971) velocity fluctuation spectral data gathered in mercury flow in a pipe. Only at the lowest Reynolds number available from Gardner & Lykoudis (10300) did the criteria indicate any attenuation could be present. Since the lowest Reynolds number presented here is approximately 2·5 times higher than the lowest one from Gardner & Lykoudis (which was only slightly affected), and also since the results

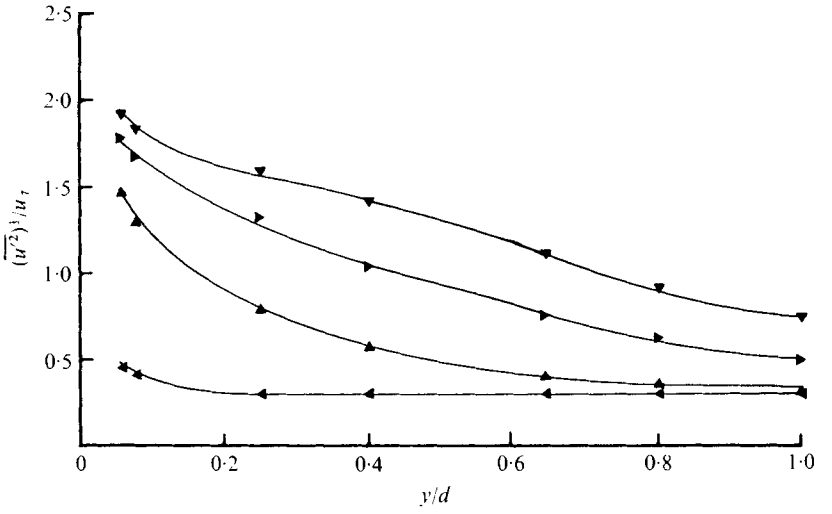

FIGURE 15. Present axial MFM turbulence intensity profiles, $Re = 53000$. $(M/Re) \times 10^4$: ◀, 32·8; ▲, 19·0; ▶, 10·7; ▼, 0.

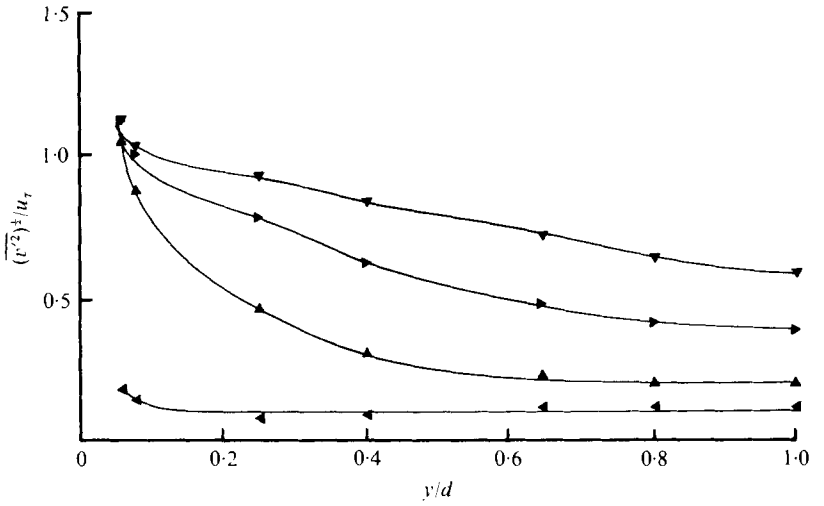

FIGURE 16. Present transverse MFM turbulence intensity profiles, $Re = 53000$. $(M/Re) \times 10^4$: ◀, 32·8; ▲, 19·0; ▶, 10·7; ▼, 0.

compare very favourably with other well known data, figures 12 and 20, the present results are considered to be free from any amplitude attenuation or phase lag effects.

MFM results. Figures 13 to 18 show the profiles of both turbulence intensity quantities $(\overline{u'^2})^{\frac{1}{2}}$ and $(\overline{v'^2})^{\frac{1}{2}}$ as a function of M/Re for each of the Reynolds numbers. The suppression of the turbulence by the magnetic field is, of course, the dominant feature of the curves. Also a dominant characteristic of the data is the finite level of the turbulence intensity (both $(\overline{u'^2})^{\frac{1}{2}}$ and $(\overline{v'^2})^{\frac{1}{2}}$) at high values of the magnetic field. Very high values of M/Re ($> 30 \times 10^{-4}$) were not used in the present experiment; this was because some data at these high values of M/Re were taken at $Re = 53000$ (figures 15 and 16) and no significant variation in the turbulence quantities was observed

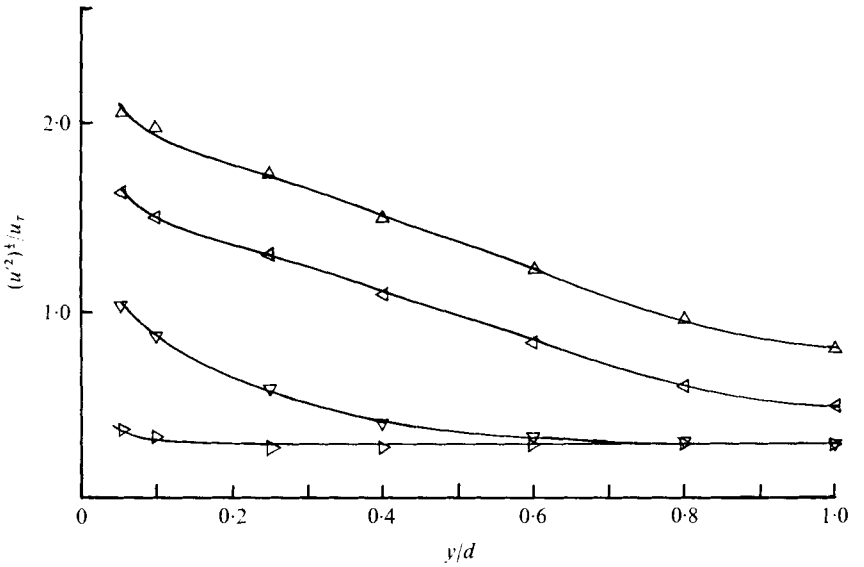

FIGURE 17. Present axial MFM turbulence intensity profiles, $Re = 102000$. $(M/Re) \times 10^4$: △, 0; ◁, 7·1; ▽, 17·1; ▷, 30·2.

across the cross-section. It was Hua (1968) who found that even at very high values of M/Re, the turbulence was not completely suppressed,† and essentially the same behaviour was observed here, figure 19. Branover, Gel'fgat, Kit & Tsinober (1970), using the conduction anemometer, found the same persistence of a low level of turbulence intensity. It should also be mentioned that both Hua (1968) and Branover *et al.* (1970) found a local minimum near $(M/Re) \times 10^4 \simeq 20$ in the curves of $(\overline{u'^2})^{\frac{1}{2}}$ *vs.* M/Re. While Hua offered no explanation, Branover offered a short discussion which involved the cascade of energy through the spectrum occurring simultaneously with the convection of fluctuation energy from upstream of the magnetic field. If convection from outside the magnetic field is to be seriously considered, a more thorough experiment will have to be performed which will conclusively demonstrate the entrance length required not only from the point of view of the pressure distribution, but also that required by the fluctuation. The recent work of Branover & Gershon (1975) casts more light in this discussion.

3.4. *Reynolds stress profiles*

OFM results. The Reynolds stresses are, of course, the most important data presented here. There are two reasons for this. First, they have been the most difficult to measure,

† Gardner (1969), who made measurements in a pipe, barely measured a relative minimum in the centre-line axial turbulence intensity as the magnetic field was increased. He used a Thermosystems model 1060 r.m.s. meter which could measure frequencies down to 0·1 hertz and had a corresponding time constant of 100 seconds. Hua (1968) used a Balentine model 320A r.m.s. meter. However, he placed a capacitor in parallel with the meter readout. The scale of the meter was not linear, however, but logarithmic. The capacitor was averaging a logarithmic signal, which is not equal to the logarithm of the average signal. The present data were reduced, as previously stated, using record lengths of 600 seconds and an electronic squaring circuit.

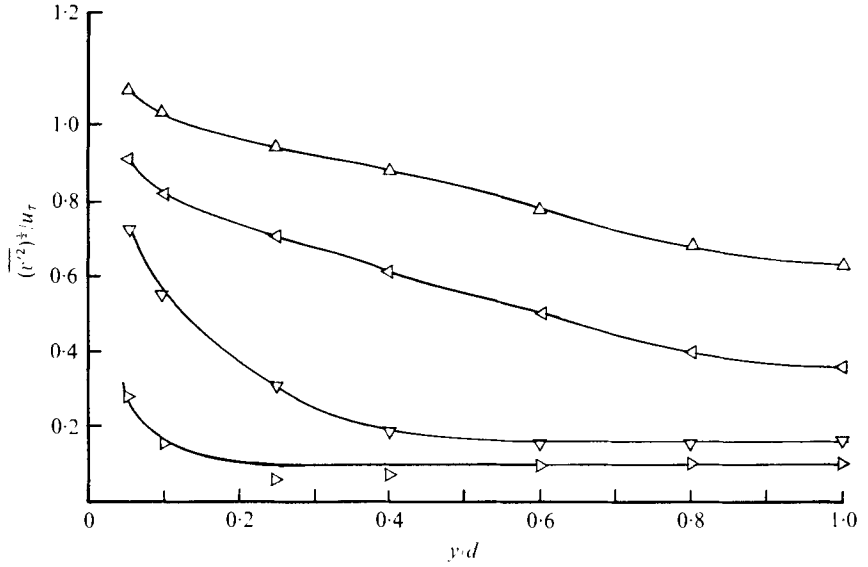

FIGURE 18. Present transverse MFM turbulence intensity profiles, $Re = 102000$. $(M/Re) \times 10^4$: △, 0; ◁, 7·1; ▽, 17·1; ▷, 30·2.

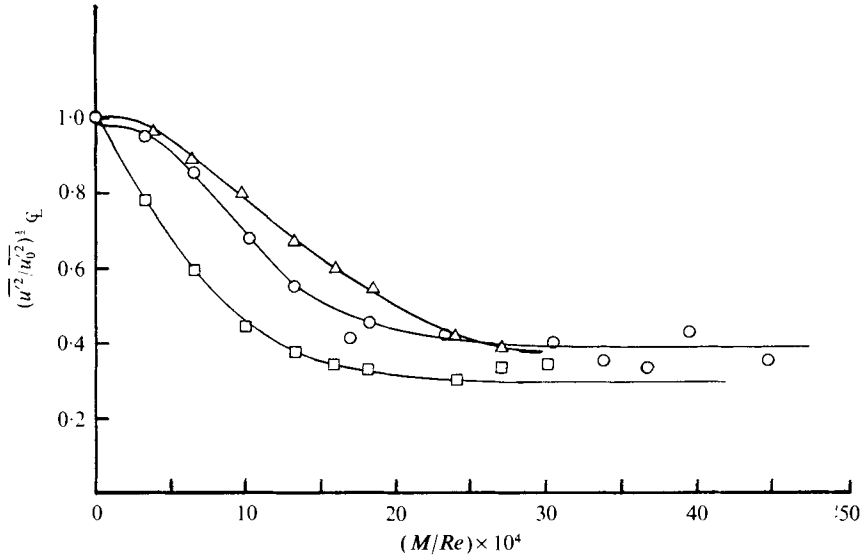

FIGURE 19. Suppression of centre-line axial turbulence intensity with increasing magnetic field. *Re*: △, 25000; ○, 53000; □, 102000.

and second, they appear explicitly in the momentum equation. With shear stress measurements in hand, most of the current MFM theories can be tested in a meaningful and decisive way. The $\overline{u'v'}$ data can also provide strong guidance in efforts to understand and construct a physically sound theory of MFM shear turbulence. By careful study of the MFM turbulence intensity data and, more important, the MFM turbulence shear stress data, the mechanism of the suppression of turbulence by a magnetic field can be determined and understood.

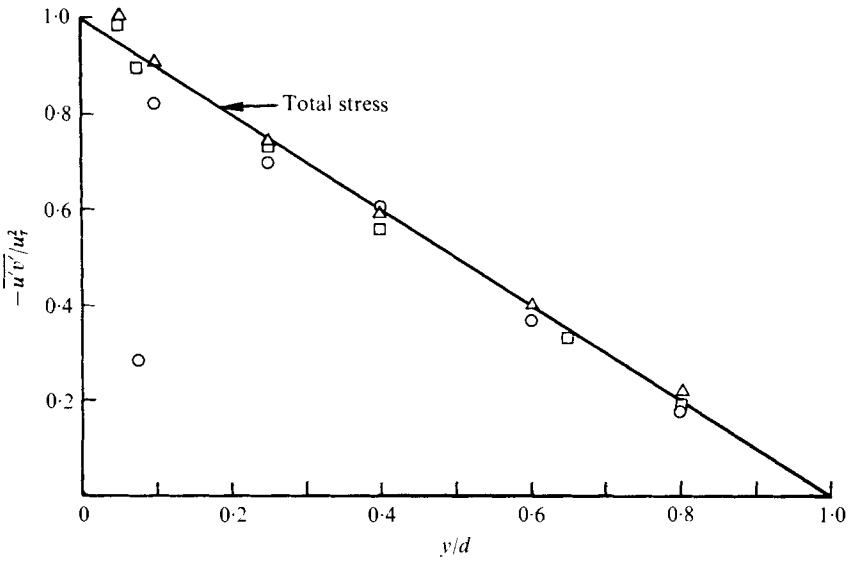

FIGURE 20. Present OFM turbulent shear stress profiles.
Re: △, 102000; □, 53000; ○, 25000.

The Reynolds stress distribution for each of the three Reynolds numbers for zero magnetic field is shown in figure 20. The total stress distribution, calculated knowing the Reynolds number, is shown as the solid line. This measurement is the first measurement in this experiment of a fluctuating quantity which can be theoretically checked. The total stress is virtually identically equal to the turbulent stress for all $y/d \gtrsim 0{\cdot}1$, depending on the Reynolds number. It is seen that the Reynolds stress measurements presented are quite good indeed. Owing to the manner in which the fluctuating data were obtained, high accuracy in the $\overline{u'v'}$ data implies high accuracy in the u' and v' measurements separately. This good correlation, once again, provided the confidence necessary to proceed with the MFM Reynolds stress measurements.

MFM results. The MFM shear stress distributions appear in figures 21 to 23. These are believed to be the first measurements of this quantity in the presence of a transverse magnetic field. Several points bear mentioning. At zero magnetic field the Reynolds stress distribution is virtually a linear relationship. Its value is zero at the channel centre-line and zero at the wall. If, however, we do not consider the region very close to the wall ($y^* > 50$), the extrapolation of the Reynolds stress distribution intersects the axis of ordinates at $-\overline{u'v'}/u_\tau^2 = 1$. Essentially, this is equivalent to saying that the total shear stress distribution is practically equal to the turbulent shear stress with the exception of the region very near the wall. It can be seen that the damping of $\overline{u'v'}$ by the magnetic field is not independent of y/d.

As mentioned earlier, the closest approach to the wall that could be made in this experiment was approximately $y^* = 40$. In this position, the X-array sensors extended a distance of approximately $y^* = 35$ in the y direction on either side of $y^* = 40$. Therefore, measurements closer to the wall could not be made. As the magnetic field becomes higher and higher, the steep velocity gradient moves closer and closer to the wall, and since turbulent production and the highest level of tur-

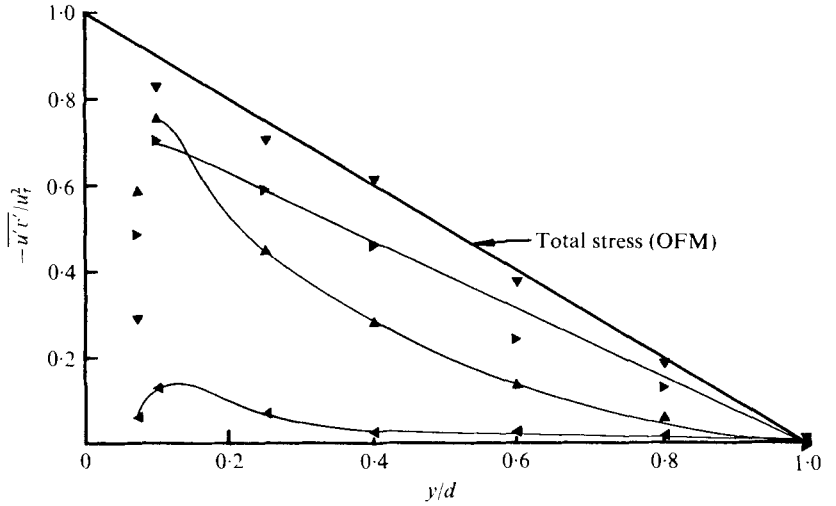

FIGURE 21. Present MFM turbulent shear stress profiles, $Re = 25000$. $(M/Re) \times 10^4$: ▼, 0; ▶, 10·8; ▲, 20·7; ◀, 36·3.

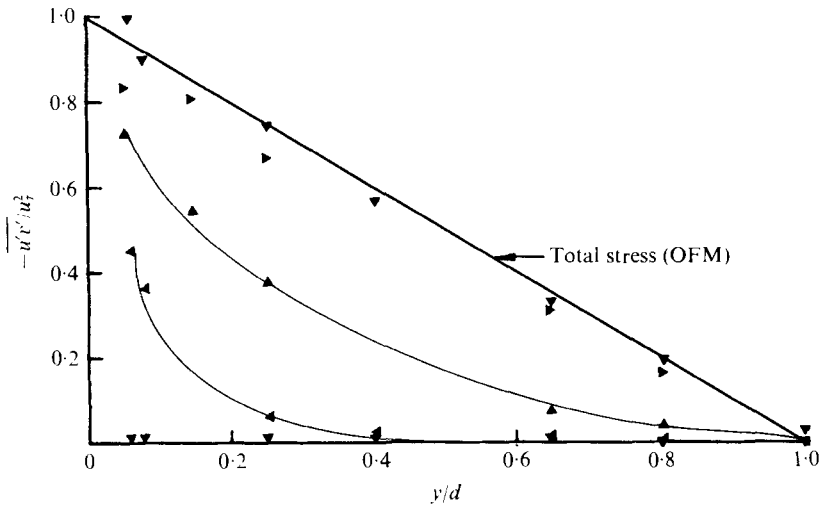

FIGURE 22. Present MFM turbulent shear stress profiles, $Re = 53000$. $(M/Re) \times 10^4$: ▼, 0; ▶, 3·6; ▲, 13·9; ◀, 25·3; ▼, 32·8.

bulence intensity are associated with these steep gradients, the peak in the turbulent shear stress moves closer and closer to the wall. This being the case, it cannot be said that the shear stress everywhere was zero at, say, the highest field shown in the figures.

The Reynolds stress profiles for $Re = 25000$ have a behaviour near the wall which is different from those of the two higher Reynolds number data. The near wall measurements of $\overline{u'v'}$ increase in magnitude as the magnetic field is increased up to a value of $(M/Re) \times 10^4 \simeq 18$ at which point they begin to decrease. This is certainly contradictory behaviour because, as we have mentioned, other authors have measured skin friction near this Reynolds number and found that C_f is decreasing up to values of

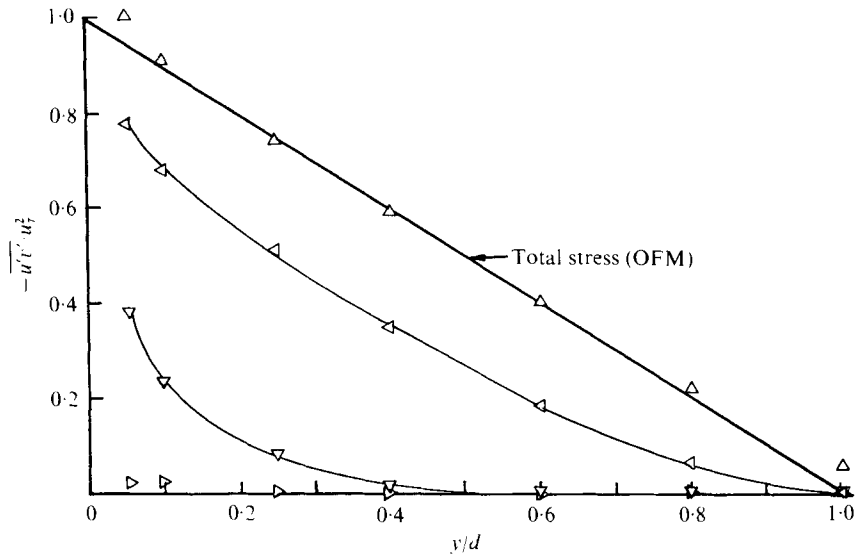

FIGURE 23. Present MFM turbulent shear stress profiles, $Re = 102000$. $(M/Re) \times 10^4$: △, 0; ◁, 7·1; ▽, 17·1; ▷, 30·2.

$(M/Re) \times 10^4 \simeq 18$. This C_f behaviour indicates that the turbulence suppression is decreasing C_f more effectively than the Hartmann flattening is increasing it. The trends in the C_f are well established, and therefore the $\overline{u'v'}$ measurements nearest the wall for $Re = 25000$ must be rejected as having experimental error in them.

4. Conclusions

The experimental results presented in this paper have attempted to clarify the behaviour of the variation of the skin friction coefficient with increasing magnetic fields. The experimental data reconfirmed the disappearance of the minimum in the family of C_f curves at low values of M/Re, as the Reynolds number is increased. The minimum was observed to disappear in the neighbourhood of $Re \simeq 100000$. The exact Re is very difficult to locate because of the nature of the measurements required to determine C_f. It was not until recently that investigators in the Soviet Union acknowledged the existence of the minimum (Branover *et al.* 1969).

The local maximum in C_f (a 'hump') which occurs in the vicinity of $(M/Re) \times 10^4 \simeq 20$, first detected by Hua (1968), was also found in the present data. Through careful measurements, the local maximum and subsequent minimum in C_f was explained by linking it to the rapid decrease in the Reynolds stress in this range of M/Re. This rapid decrease in Reynolds stress outweighs the Hartmann flattening effect.

The behaviour of C_f at very high values of the magnetic field strength was shown to be due to the distortion of the velocity profile in the width direction into an 'M' shape. The theoretical work of Shercliff (1956), experimental work from the Soviet Union, Bocheninski *et al.* (1971), and independent velocity profile measurements by the authors have demonstrated the existence of the 'M' shaped profiles. These profiles are certainly not consistent with the predictions of the Shercliff (1953) solution and therefore his predictions of C_f are not expected to agree with data from channels

having these velocity profiles. The 'M' shaped velocity profiles are the result of magnetic entrance effects (Shercliff 1956). If the magnetic field is not uniform in the width direction, as is the case as higher and higher field strengths are reached, the 'M' shaped profiles are accented further. The result of these distorted velocity profiles is the high M/Re behaviour of C_f observed first by Hua (1968) but unexplained until now.

For the Reynolds numbers involved in this experiment, the 'M' profiles did not influence the mean and fluctuating velocity measurements. It was found, as expected, that as the magnetic field was increased and the turbulence damped out, the laminar Hartmann velocity profiles were approached.

The measurements of the Reynolds stresses indicate that the magnetic field does act in suppressing the $\overline{u'v'}$ correlation more effectively than u' or v'. The u' and v' fluctuations were not completely suppressed by the magnetic field, even at values of $(M/Re) \times 10^4 \simeq 50$. The non-vanishing turbulence intensity was first detected by Hua (1968) and several explanations for it have been offered (Branover *et al.* 1970; Slyusarev 1971). These proposed explanations all rely to a greater or lesser extent upon the assumption that the flow within the magnetic field is not fully developed, or at least that there does exist an axial gradient of the turbulence intensity. Measurements of the turbulence intensity at several axial locations were not made in this experiment, but the axial static pressure distribution gave no indication that any gradients (other than the static pressure gradient) existed in the axial direction. The investigation of Branover & Gershon (1975) should be mentioned in this context.

Concerning a local maximum in the axial turbulence intensity as a function of M/Re, examination of figure 19 does not give a clear indication of such a maximum. It should again be pointed out that the root mean square of the turbulence intensities presented here were true r.m.s. values, the mean being integrated for a time period in excess of ten minutes. Neither Hua (1969) nor Slyusarev (1971) reported r.m.s. measurements with such a record length. It is possible that their reports of a local maximum in the turbulence intensity as a function of M/Re was due to inadequate instrumentation. The present experiment confirmed that a finite level of turbulence intensity for both u' and v' exists, even after the Reynolds stresses have been completely suppressed. Further statements about the mechanisms by which the fluctuations are sustained in the face of the magnetic field, or whether a local maximum exists, cannot be made from the present data.

The authors wish to acknowledge with gratitude the financial support of the National Science Foundation under Grant GK-23694.

REFERENCES

Bocheninski, B. E., Branover, H. H., Tanayev, A. B. & Chereyev, Yu. E. 1971 Experimental investigation of the resistance to flow of an electrically conducting fluid in plane insulated channels in a transverse magnetic field considering end effects and rough walls. *Izv. AN S.S.S.R. Mekh. Zh. i Gaza* **4**, 10–21.

Branover, H. H. 1974 On some effects in laboratory MHD flows in rectangular ducts in transverse magnetic fields. *14th Symp. Engineering Aspects of Magnetohydrodynamics*, pp. 3.1–3.4.

Branover, H. H. & Gel'fgat, Yu. M. 1968 Stabilization of plane-parallel flow in a transverse magnetic field. *Magnitnaya Gidrodynamika* **4** (3), 9.

Branover, H. H., Gel'fgat, Yu. M., Kit, L. G. & Platnicks, E. A. 1970 The effect of a

transverse magnetic field on the turbulence intensity profiles in a rectangular channel. *Magnitnaya Gidrodynamika* **6** (3), 41.

BRANOVER, H. H., GEL'FGAT, YU. M., KIT, L. G. & TSINOBER, A. B. 1970 Study of MHD turbulence in tubes using conduction anemometers. *Izv. AN S.S.S.R. Mekh. Zh. i Gaza* **5** (2), 35.

BRANOVER, H. H., GEL'FGAT, YU. M., PETERSON, D. A. & TSINOBER, A. B. 1969 Turbulent Hartmann flow. *Magnitnaya Gidrodynamika* **5** (1), 61.

BRANOVER, H. H., GEL'FGAT, YU. M. & TSINOBER, A. B. 1966 Turbulent magnetohydrodynamic flows in prismatic and cylindrical ducts. *Magnitnaya Gidrodynamika* **2** (3), 3.

BRANOVER, H. H., GEL'FGAT, YU. M., TSINOBER, A. B., SHTERN, & SHERBININ, E. V. 1966 The application of Pitot and Prandtl tubes in magnetohydrodynamics experiments. *Magnitnaya Gidrodynamika* **2** (1), 98.

BRANOVER, H. H. & GERSHON, P. 1975 An experimental MHD facility for the investigation of some important features of turbulence suppression. *MHD Flows and Turbulence* (ed. H. Branover). Wiley and Israel University Press, Jerusalem.

BROUILLETTE, E. C. 1966 Experimental and theoretical analysis of magneto-fluid-mechanic channel flow. Ph.D. thesis, Purdue University.

BROUILLETTE, E. C. & LYKOUDIS, P. S. 1963 Measurements of skin friction for turbulent magneto-fluid-mechanic channel flow. *Purdue Univ. Rep.* A & ES 62-10, August 1962. See also *Proc. 4th Symp. Engineering Aspects of MHD (I.E.E.E.)*, p. 45.

BROUILLETTE, E. C. & LYKOUDIS, P. S. 1967 Magneto-fluid-mechanic channel flow I. Experiment. *Phys. Fluids* **10**, 995.

COMTE-BELLOT, G. 1965 Turbulent flow between two parallel planes. *Publ. Sci. Tech. Min. Air*, no. 419.

GARDNER, R. A. 1969 Magneto-fluid-mechanic pipe flow in a transverse magnetic field with and without heat transfer. Ph.D. thesis, Purdue University.

GARDNER, R. A. & LYKOUDIS, P. S. 1971 Magneto-fluid-mechanic pipe flow in a transverse magnetic field. Part 1. Isothermal flow. *J. Fluid Mech.* **47**, 737.

HARTMANN, J. 1937 Hg Dynamics-I. *Kgl. Danske Videnskab Selskab Mat.-Fys. Medd.* **15**, no. 6.

HUA, H. M. 1968 Heat transfer from a constant temperature circular cylinder in cross-flow and turbulence measurements in an MFM channel. Ph.D. thesis, Purdue University.

HUNT, J. C. R. 1965 Magnetohydrodynamic flow in rectangular ducts. *J. Fluid Mech.* **21**, 577.

HUNT, J. C. R. & MOREAU, R. 1976 Liquid-metal magnetohydrodynamics with strong magnetic fields: a report on Euromech 70. *J. Fluid Mech.* **78**, 261.

LAUFER, J. 1950 Investigation of turbulent flow in a two-dimensional channel. *N.A.C.A. Tech. Note* no. 2123.

LECOCQ, P. 1964 A contribution to the study of the loss of flow and the velocity profiles for turbulent magnetohydrodynamic flow. *Bulletin du Centre de Recherches et d'Essais de Chatou*, suppl. 8.

LYKOUDIS, P. S. 1960 Transition from laminar to turbulent flow in magneto-fluid-mechanic channels. *Rev. Mod. Phys.* **32**, 796.

MACIULAITIS, A. & LOEFFLER, L. A. 1964 A theoretical investigation of MHD channel entrance flow. *A.I.A.A. J.* **2**, 2100.

MALCOLM, D. G. 1975 Hot film anemometry in liquid-metal MHD. In *MHD Flows and Turbulence, Proc. Bat-Sheva Inter. Seminar, Beersheva*, p. 119.

MALCOLM, D. G. & VERMA, V. 1973 Dynamic response of forced convective heat transfer from cylinders to low Prandlt number fluids. *Proc. 3rd Symp. Turbulence in Liquids, Univ. Missouri-Rolla*, p. 15.

MURGATROYD, W. 1953 Experiments on magneto-hydrodynamic channel flow. *Phil. Mag.* **44**, 1348.

NICKURADSE, J. 1929 *Forsch.-Arb. Geb. Ing.-Wes.* **289**.

PAPAILIOU, D. D. & LYKOUDIS, P. S. 1974 Magneto-fluid-mechanics free convection turbulent flow. *Int. J. Heat Mass Transfer* **17**, 1181.

PATRICK, R. P. 1976 MFM turbulence suppression. Ph.D. thesis, Purdue University.

REED, C. B. 1976 An investigation of shear turbulence in the presence of magnetic fields. Ph.D. thesis, Purdue University.

REED, C. B. & LYKOUDIS, P. S. 1977 Turbulence measurements in mercury under the influence of a magnetic field. *Proc. 5th Biennial Symp. Turbulence, Univ. Missouri-Rolla*, session V, p. 1.

SCHLICHTING, H. 1960 *Boundary Layer Theory*. 4th edn. p. 515. Pergamon.

SHERCLIFF, J. A. 1953 Steady motion of conducting fluids in pipes under transverse magnetic fields, *Proc. Camb. Phil. Soc.* **49**, 136.

SHERCLIFF, J. A. 1956 Edge effects in electromagnetic flowmeters. *J. Nuclear Energy I* **3**, 305.

SLEICHER, C. A. & LIM, G. B. 1973 Measurement of unsteady flows in mercury with hot-film anemometers. *Proc. 3rd Symp. Turbulence in Liquids, Univ. Missouri-Rolla*, p. 1.

SLYUSAREV, N. M. 1971 Effect of a transverse magnetic field on turbulent channel flows *Magnitnaya Gidrodynamica* **7** (1), 18.